



# Shape analysis of the StW 578 calotte from Jacovec Cavern, Gauteng (South Africa)

## AUTHORS:

Amélie Beaudet<sup>1,2,3</sup>   
Jean Dumoncel<sup>4</sup>   
Jason L. Heaton<sup>5,6,7</sup>   
Travis R. Pickering<sup>5,7,8</sup>   
Ronald J. Clarke<sup>9</sup>   
Kristian J. Carlson<sup>9,8</sup>   
Lunga Bam<sup>10</sup>  
Luc Van Hoorebeke<sup>11</sup>   
Dominic Stratford<sup>2</sup>

## AFFILIATIONS:

<sup>1</sup>Department of Archaeology, University of Cambridge, Cambridge, United Kingdom  
<sup>2</sup>School of Geography, Archaeology and Environmental Studies, University of the Witwatersrand, Johannesburg, South Africa  
<sup>3</sup>Catalan Institute of Palaeontology Miquel Crusafont, Autonomous University of Barcelona, Barcelona, Spain  
<sup>4</sup>French National Centre for Scientific Research (CNRS), Paris, France  
<sup>5</sup>Department of Biology, Birmingham-Southern College, Birmingham, Alabama, USA  
<sup>6</sup>Evolutionary Studies Institute, University of the Witwatersrand, Johannesburg, South Africa  
<sup>7</sup>Plio-Pleistocene Palaeontology Section, Department of Vertebrates, Ditsong National Museum of Natural History, Pretoria, South Africa  
<sup>8</sup>Department of Anthropology, University of Wisconsin-Madison, Madison, Wisconsin, USA  
<sup>9</sup>Department of Integrative Anatomical Sciences, Keck School of Medicine, University of Southern California, California, USA  
<sup>10</sup>South African Nuclear Energy Corporation (Necsa), Pelindaba, South Africa  
<sup>11</sup>UGT Department of Physics and Astronomy, Ghent University, Ghent, Belgium

## CORRESPONDENCE TO:

Amélie Beaudet

## EMAIL:

beaudet.amelie@gmail.com

## DATES:

Received: 14 July 2021

Revised: 06 Oct 2021

Accepted: 01 Oct. 2021

Published: 29 Mar. 2022

## HOW TO CITE:

Beaudet A, Dumoncel J, Heaton JL, Pickering TR, Clarke RJ, Carlson KJ, et al. Shape analysis of the StW 578 calotte from Jacovec Cavern, Gauteng (South Africa). *S Afr J Sci.* 2022;118(3/4), Art. #11743. <https://doi.org/10.17159/sajs.2022/11743>

## ARTICLE INCLUDES:

- Peer review
- Supplementary material

## DATA AVAILABILITY:

- Open data set
- All data included
- On request from author(s)
- Not available
- Not applicable

The fossiliferous deposits within the lower-lying Jacovec Cavern in the locality of Sterkfontein yielded valuable hominin remains, including the StW 578 specimen. Because StW 578 mainly preserves the calotte, the taxonomic status of this specimen has been a matter of discussion. Within this context, here we employed high-resolution microtomography and a landmark-free registration method to explore taxonomically diagnostic features in the external surface of the StW 578 calotte. Our comparative sample included adult humans and common chimpanzees as well as one *Australopithecus africanus* specimen (Sts 5). We partially restored the StW 578 calotte digitally and compared it to extant specimens and Sts 5 using a landmark-free registration based on smooth and invertible surface deformation. Our comparative shape analysis reveals morphological differences with extant humans, especially in the frontal bones, and with extant chimpanzees, as well as intriguing specificities in the morphology of the StW 578 parietal bones. Lastly, our study suggests morphological proximity between StW 578 and Sts 5. Given the intimate relationship between the brain and the braincase, as well as the integration of the hominin face and neurocranium, we suggest that cranial vault shape differences between StW 578 and extant humans, if confirmed by further analyses, could be either explained by differences in brain surface morphology or in the face. Besides providing additional information about the morphology of the Jacovec calotte that will be useful in future taxonomic discussion, this study introduces a new protocol for the landmark-free analysis of fossil hominin cranial shape.

## Significance:

- We provide further information on the enigmatic fossil specimen StW 578.
- We introduce a new approach for the morphological study of fossil hominin crania.
- We highlight morphological similarities between StW 578 and 'Mrs Ples'.

## Introduction

The palaeocave infills of the Sterkfontein Caves, which lie 50 km northwest of Johannesburg (South Africa), are well known for having yielded iconic fossil specimens, such as Sts 5 ('Mrs Ples') and StW 573 ('Little Foot').<sup>1</sup> Fossiliferous deposits within the lower-lying Jacovec Cavern have provided additional hominin remains that are of particular interest; prominent among them is the StW 578 cranium.<sup>2</sup> StW 578 was discovered in 1995 partly in situ in 'Orange' sediments (Lo27 coordinates: Y, -73582.548; X, 2878771.407; Z, 1450.909) that are composed of partially calcified breccia exposed in the roof of the eastern part of the Jacovec Cavern<sup>2</sup>, and partly in collapsed breccia beneath. Because of the conflicting geomorphological scenarios of the infilling of the lower chambers in Sterkfontein<sup>2,3-7</sup>, determining a geological age for StW 578 is particularly challenging<sup>2,8-11</sup>. Absolute dating using cosmogenic nuclide burial methods originally provided an age of 4.02±0.27 Ma for the cranium.<sup>2</sup>

Together with the 3.67-million-year-old skeleton of StW 573, StW 578 represents some of the oldest evidence of human evolution in southern Africa.<sup>12</sup> Because of its late Pliocene age, the StW 578 calotte (i.e. the top part of the cranium) is of great interest for reconstructing early hominin evolution. Late Pliocene fossiliferous deposits in the Jacovec Cavern coincide with an important radiation of the genus *Australopithecus*, with the emergence of *Australopithecus afarensis*, *Australopithecus deyiremeda*, *Australopithecus bahrelghazali* and the 'Burtele Foot'.<sup>13</sup> For instance, previous studies of the postcranial assemblage from the Jacovec Cavern revealed an interesting mosaic of features, with the femur having a very long neck relative to a small head but a round-sectioned shaft, and with a clavicle (StW 606) that has morphological similarities to extant chimpanzees.<sup>2,14</sup> Accordingly, StW 578 has the potential to contribute to our understanding of morphological variation and taxonomic diversity within *Australopithecus* in the late Pliocene.

Because the Jacovec cranium mainly preserves part of the calotte (Figure 1), along with fragments of the face and dentition, and a temporal bone (see Partridge et al.<sup>2</sup>; all initially cleaned and reconstructed by RJ Clarke), the taxonomic status of this specimen has been a matter of discussion. Indeed, in the original description, the authors refrained from attributing StW 578 to any species.<sup>2</sup> Study of the cranial vault thickness and composition revealed close affinities with the *Australopithecus* specimens from Sterkfontein Member 4.<sup>8</sup> However, Partridge et al. noticed that:

*posterior to this fossa the tympanic plate slopes strongly posteriorly as it does in Pan, and in this respect differs from all other Australopithecus temporals from Sterkfontein Member 4, which resemble more closely the human, vertically inclined tympanic plate.*<sup>2(p.609)</sup>

The dental and facial morphology and the presence of a metopic ridge on the frontal convinced Clarke and Kuman<sup>12</sup> to classify this specimen as *Australopithecus africanus* rather than *Australopithecus prometheus*, teeth of which also occur in the Jacovec sample.

**EDITORS:**Margaret Avery   
Jemma Finch **KEYWORDS:***Australopithecus*, Sterkfontein Caves, cranial morphology, surface-based comparison**FUNDING:**

DSI-NRF, University of the Witwatersrand, AESOP+ program, Claude Leon Foundation, DSI-NRF Centre of Excellence in Palaeosciences, French Institute of South Africa, The Ghent University Special Research Fund (BOF EXP2017.0007), South African National Research Foundation (grant numbers 82591, 82611, 98808, 129336), PAST

Given the significance of this specimen and ongoing debates, we virtually reconstructed the StW 578 calotte and compared its shape to those of extant humans, extant chimpanzees, and *Australopithecus africanus* (as represented by Sts 5). Besides introducing a new protocol for the shape analysis of fossil hominin crania, we also provide new insights into the morphology of the Jacovec specimen.

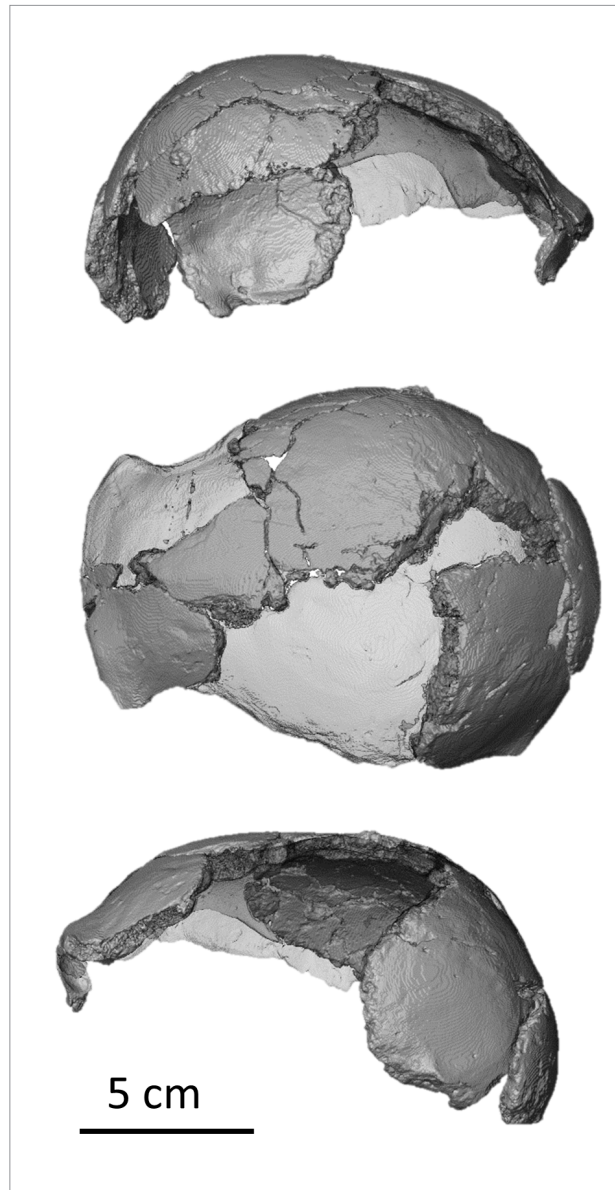


**Figure 1:** Virtual rendering of the StW 578 calotte in lateral right (top), superior (middle) and lateral left (bottom) views. Plaster used to physically reconstruct the cranium is in light grey and transparent.

## Material and methods

### **Comparative material**

Our comparative sample of extant specimens comprised mixed-sex samples of non-pathological adult humans (*Homo sapiens*,  $n=6$ ) and common chimpanzees (*Pan troglodytes*,  $n=6$ ). Extant human samples were obtained from the Pretoria Bone Collection of the University of Pretoria<sup>15</sup> while extant chimpanzee samples were obtained from the Royal Museum for Central Africa in Tervuren (Belgium). Additionally, we included the *Australopithecus africanus* specimen Sts 5 that comes from Sterkfontein Member 4, dated to about 2.8–2.4 Ma based on faunal assemblages.<sup>16–20</sup> Sts 5 is currently housed in the Ditsong National Museum of Natural History (South Africa). Parts of the outer bone table of Sts 5 remained in the breccia during the initial preparation by Broom<sup>17,21</sup>, but this does not alter the overall shape of the cranial vault.

### **Scanning and pre-processing step**

StW 578 and Sts 5 were scanned at the microfocuss X-ray tomography facility of the Palaeosciences Centre at the University of the Witwatersrand, in Johannesburg (South Africa), at a spatial resolution of 66.6  $\mu\text{m}$  and 75.0  $\mu\text{m}$  (isotropic voxel size), respectively. A 3D model of StW 578 is available on MorphoSource<sup>22</sup>. Extant humans and

chimpanzees have been similarly scanned at the South African Nuclear Energy Corporation in Pelindaba, South Africa, and at the Centre for X-ray Tomography of Ghent University (UGCT) in Ghent, Belgium, with a resolution ranging from 70.0  $\mu\text{m}$  to 102.3  $\mu\text{m}$ .

As a pre-processing step, all of the crania were oriented the same way with the opisthocranium and glabella aligned on a single transverse plane, and a new image stack reflecting the standardised orientation was generated using Avizo v9.0<sup>23</sup> (FEI Visualization Sciences Group Inc., <https://www.fei.com/software/amira-avizo/>)<sup>8</sup>. The same transverse plane was used to virtually cut the crania so that the superior part of the braincase (that is preserved in StW 578) could be separated from the rest of the cranium and studied. Finally, because we were interested in the external shape of the cranium only, we virtually isolated the external surface from the inner surface.

### Reconstruction of StW 578

Before virtually reconstructing the StW 578 calotte, we removed the plaster using segmentation tools in Avizo v9.0 (STEP1, Figure 2A). We fitted a surface through StW 578 using the tool 'Patch' in Rhinoceros 3D v6.0<sup>24</sup> (STEP2, Figure 2B). The resulting surface (Figure 2B) was opened in Avizo v9.0 and the parts of the new surface that filled in the gaps between bones were manually extracted (Figure 2C) and merged with the initial surface using the tool 'Flatten visible layer' in Meshlab<sup>25</sup> (STEP3, Figures 2D,E). This new surface was mirrored to reconstruct missing regions in the opposite side (Figure 2F). Finally, STEP2 and STEP3 were repeated (Figure 2G,H). Inferior portions of the parietal and frontal bones were still missing at this stage (Figure 2E). Because these regions cannot be reconstructed using existing bones, we preferred not to estimate them and thus systematically removed the homologous regions in all comparative specimens (see below).

Similarly, we removed the plaster in Sts 5 and the missing regions were virtually filled in by applying STEP2 and STEP3.

### Shape analysis

We compared StW 578 to extant specimens and Sts 5 by using landmark-free registration based on smooth and invertible surface deformation.<sup>26-30</sup> This approach has been previously applied to a number of craniodental and postcranial structures, including endocasts<sup>27,29</sup>, enamel-dentine junctions<sup>28,31</sup>, vertebrae<sup>32</sup> and bony labyrinths<sup>33</sup> and comparisons between the landmark-based and landmark-free approaches have revealed the ability of the latter approach for capturing geometric details and for statistical determination of geometric correspondence<sup>34</sup>. Because the StW 578 calotte is partial, instead of using the whole surface to align specimens as in previous studies<sup>27-29</sup>, we used four landmarks, i.e. glabella, opisthocranium, and two landmarks positioned on the external surfaces of the right and left parietal bones at the intersection of (1) a coronal plane positioned at three-quarters of the maximum length of the calotte and of (2) the transverse plane that was used for isolating the top of the calotte. Surfaces were aligned in position, orientation and scale using one surface that was randomly selected as a reference and by using the tool 'Landmark Surface Warp' (method: Rigid + Uniform Scale) in Avizo v9.0 which is based on the iterative closest point algorithm that minimises the root mean square distance between the points of each specimen to corresponding points on the reference.<sup>35</sup> A template was deformed to extant specimens using Deformetrica v4.<sup>26,36,37</sup> The extant specimens and Sts 5 were deformed to StW 578. Based on this computation, the parts of the frontal and parietal bones that are missing in StW 578 (Figure 2E) were systematically removed from the comparative extant and fossil specimens using an automated method.<sup>29,30,36</sup> We then deformed another template to the extant comparative surfaces generated after this step and a global mean shape as well as taxon-specific mean shapes (*Homo sapiens* and *Pan troglodytes*, each  $n=6$ ) were generated. Finally, the global mean shape and taxon mean shapes were deformed to StW 578 and Sts 5. The resulting 3D deformation fields that integrate local orientation and the amplitude of the deformation were analysed using principal component analysis (PCA) (Figure 3). Displacements from the taxon mean shapes to StW 578 and from Sts 5 to StW 578 were rendered by colour maps.

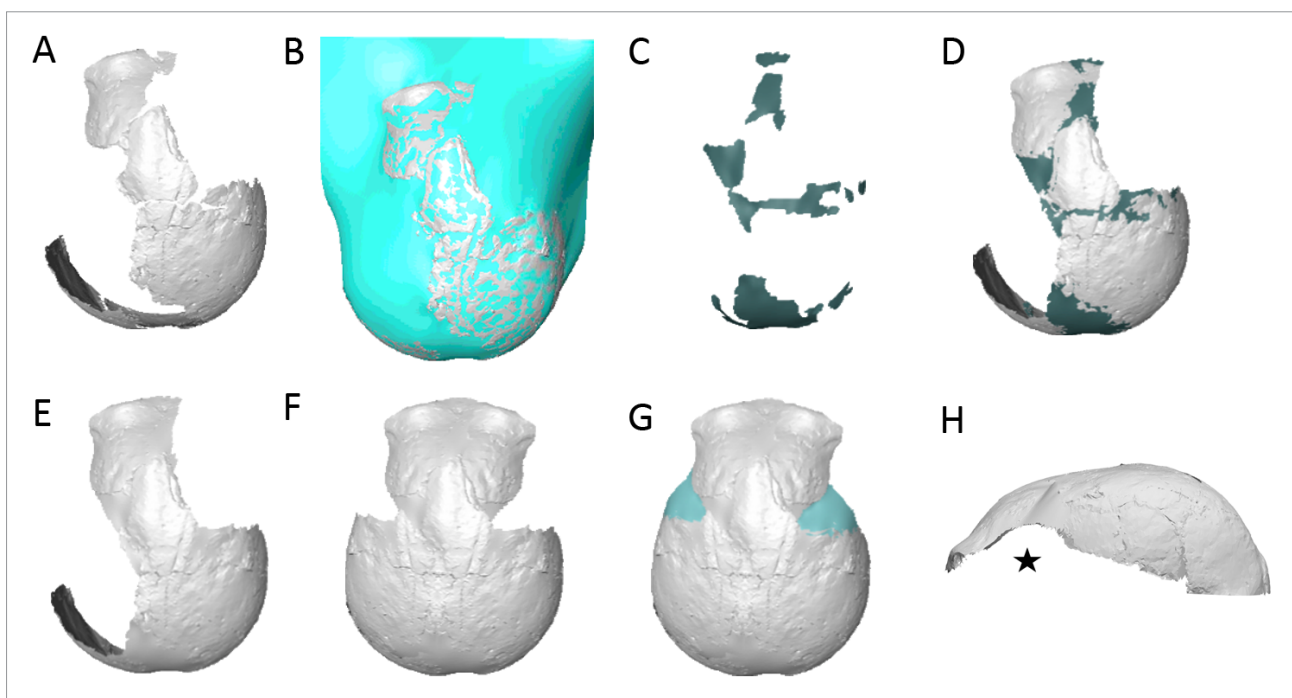


**Figure 2:** Successive steps for the virtual reconstruction of the StW 578 cranium. The initial surface (A) has been wrapped using a patch (B) and the gaps reconstructed (C) and merged with the initial surface (D). To the end result of the first iteration (E), a mirror was applied (F) and the overall process repeated (G). The resulting surface is lacking lateral portions of the frontal and parietal bones (H) indicated by a star.

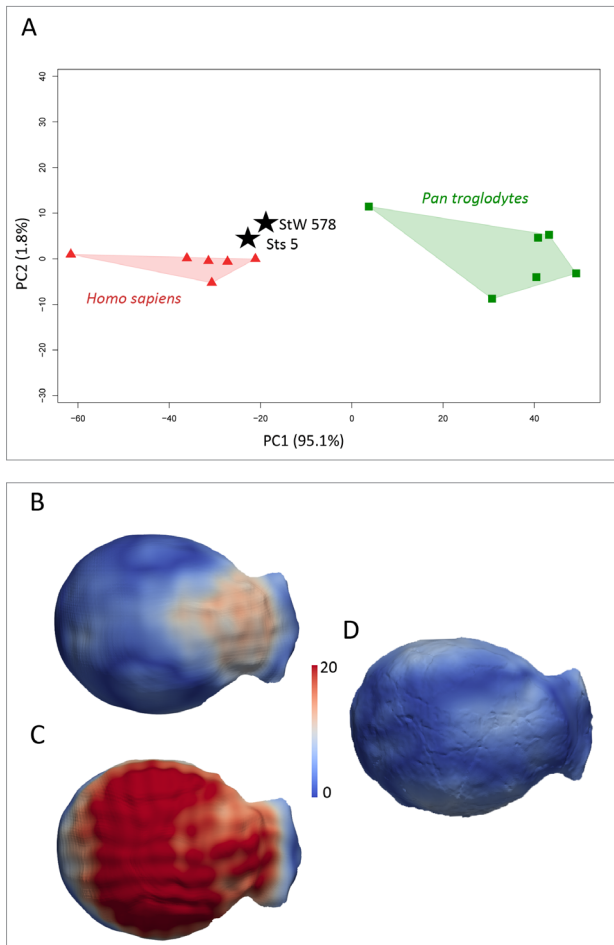


**Figure 3:** Principal component (PC) analysis of the deformation-based shape comparisons of the StW 578 and Sts 5 calottes and of the extant human and chimpanzee calottes (A). Comparative maps of morphological deformations from the taxon-specific mean shapes computed for extant humans (B) and extant chimpanzees (C) to StW 578 and from Sts 5 to StW 578 (D) in superior view. The colour bar represents the number of deformations.

To estimate potential bias induced by our reconstruction of StW 578 (Figure 2) in the shape analysis, we computed a second set of deformations using the original surface of the StW 578 calotte (i.e. not reconstructed, neither physically nor virtually). The regions that correspond to the missing bone in StW 578 were automatically removed from the extant specimens by using the results of the first set of deformations.<sup>29,36</sup> We then computed a PCA using the deformation fields generated by this second set of deformation (Figure 4).

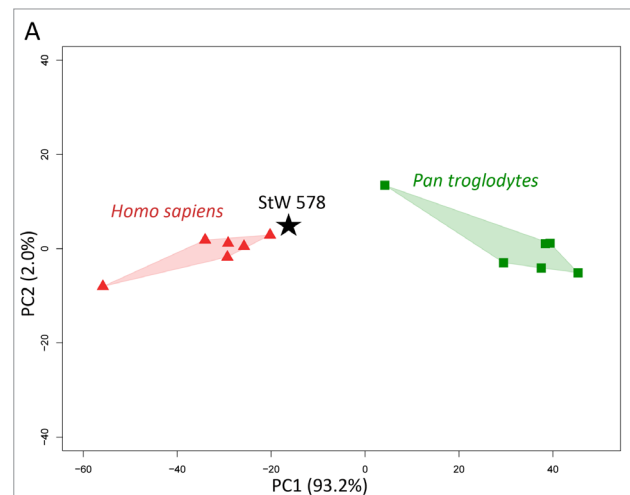
## Results

Figure 3A shows the PCA of the deformation-based shape comparison of StW 578 and extant and fossil comparative specimens. The two extant comparative groups are well discriminated along PC1, which accounts for 95.0% of the variation. Chimpanzees plot in positive space while extant humans plot in negative space. Along PC1, both StW 578 and Sts 5 plot close to each other and closer to the extant human cluster in negative space. Along PC2, which represents 1.8% of the variation, the two comparative groups and the fossil specimens mostly overlap.

The nature and extent of the differences between StW 578 and the comparative specimens were investigated using topological mapping of interspecific variation (Figure 3B–D). Compared with extant humans, the lateral part of the parietal bones in StW 578 is slightly more elevated as indicated by the white spots on both sides of the cranial vault in Figure 3B. On the contrary, the frontal bones in StW 578 are more flattened than

in extant humans (in which the rounded forehead contributes to the globular aspect of the overall cranium) as emphasised by the large pink to red area in the colour maps. Compared with the extant chimpanzees, the parietal and frontal bones of the StW 578 calotte are significantly more elevated, which is shown in Figure 3C by the cranial vault being nearly entirely red. The shapes of the external surfaces of the tops of the calottes of StW 578 and Sts 5 are closely similar (Figure 3D), with only minimal differences in the superior part of the frontal bone and the lateral surface of the parietal bones.

Finally, we investigated how our virtual reconstruction of StW 578 may influence our shape analysis by applying the same protocol to the bones preserved in the original specimen and comparing the morphology to the extant groups. If we consider the results of the deformation-based shape comparison of the regions of the calotte that are preserved in StW 578 and artificially isolated in the extant comparative sample (Figure 4), StW 578 plots closer to the extant human cluster along PC1 that represents 93.2% of the variation. Here again, StW 578, extant humans and extant chimpanzees overlap along PC2 that represents 2.0% of the variation. We thus obtain similar results as in the first set of deformation that includes our reconstruction of the calotte, which tends to suggest that our reconstruction does not bias the result of the shape analysis.



**Figure 4:** Principal component (PC) analysis of the deformation-based shape comparisons of the unreconstructed upper part of the StW 578 calotte and of the extant human and chimpanzee calottes, focusing on bones originally preserved in StW 578 and artificially isolated in the comparative sample.

## Discussion

Because of its fragmentary nature, the taxonomic and phylogenetic status of the StW 578 calotte remains debatable, although it has been recently assigned to *A. africanus* by Clarke and Kuman<sup>12</sup>. Within the limits of our sample, our comparative shape analysis reveals morphological differences with the cranial vault of extant humans, mainly located in the frontal bones and on the lateral surface of the parietal bones, and more dramatically with the cranial vault of extant chimpanzees. As such, our study further clarifies the polarity (i.e. derived or ancestral) of the cranial features identified in StW 578.<sup>2</sup>

The hominin cranium is highly integrated.<sup>38</sup> Frontal bone morphology reflects the integration of the bone structures of the upper face and anterior neurocranium.<sup>39</sup> Within this context, the marked differences identified in the frontal bones of StW 578 and extant humans by our comparative shape analysis might reflect the primitive morphology of the upper face in *Australopithecus*. Indeed, the hominin face has experienced dramatic changes through time, with the earliest changes affecting primarily the canines and supraorbital regions (potentially associated to social interactions) and later modifications related to the masticatory apparatus and a transition from tough and hard to soft or pre-processed food.<sup>40</sup> On the other hand, within the frame of the hypothesis



of modularity of the hominin face and neurocranium, we might consider the possibility that differences in the frontal bone could be the result of neutral evolution.<sup>41,42</sup> Alternatively, this result might be explained by the influence of the frontal and temporal lobes on the morphology of the frontal bones.<sup>43</sup> However, because significant reorganisation of the frontal and temporal lobes occurred in later hominins<sup>44,45</sup>, this hypothesis is unlikely. Lastly, it is noteworthy that the extant human frontal bones are characterised by the presence of two bosses which are absent in fossil hominins.<sup>46</sup> Nonetheless, these results are preliminary and will need to be further supported by future analyses including a large extant human sample.

The assessment of the cranial vault thickness variation in StW 578 demonstrated particularly thick parietal bones, which differs from the pattern of cranial thickness reported for extant humans and extant chimpanzees (see Fig. 8 in Beaudet et al.<sup>8</sup>). The growth and development of the neurocranial bones is closely related to the growth and development of the brain (within the frame of the functional matrix hypothesis<sup>47</sup>). Accordingly, we might hypothesise that differences in brain development and growth between StW 578 and extant humans could explain differences in the external cranial shape. Alternatively, it has been hypothesised that cranial vault bones may adapt to empty space and become thicker.<sup>48</sup> Consequently, thickened bone in the parietal region<sup>9</sup> and the resulting shape of the external surface of the braincase in StW 578 (this study) could be related to the morphology of the brain, and the lack of parietal expansion that is specifically found in modern human brains.<sup>49</sup>

Finally, our study reveals close affinities of the shape of the external surface of the calotte of StW 578 and the *Australopithecus africanus* specimen Sts 5. At this stage, no conclusions on the taxonomic status of StW 578 could be drawn, as our sample, besides being relatively small, did not include any representatives of the taxon *Australopithecus prometheus*.<sup>12</sup> However, unlike what is seen in the tympanic plate<sup>2</sup>, our study of the external morphology of the StW 578 calotte does not reveal any substantial differences with another *Australopithecus* specimen, Sts 5, nor distinct proximity with extant chimpanzees. However, given the fact that the present preliminary results derive from a new protocol, our results should be carefully considered and future analyses should help clarify this question.

## Acknowledgements

We are indebted to E. Gillisen and W. Wendelen (Tervuren), G. Krüger and E. L'Abbé (Pretoria), L. Kgasi, H. Fourie and S. Potze (Pretoria), and S. Jirah and B. Zipfel (Johannesburg) for granting us access to fossil and comparative material in their care. We also thank J. Hoffman and F. de Beer (Pelindaba), and M. Dierick (Ghent) for X-ray microtomographic acquisitions. We are grateful to the Ditsong National Museum of Natural History and the University of the Witwatersrand for loaning hominin crania in their collections. For technical and/or scientific discussion/collaboration we are grateful to: M. Carmen Arriaza (Johannesburg), G. Krüger (Pretoria), K. Kuman (Johannesburg), E. L'Abbé (Pretoria), A. Oettlé (Pretoria) and J.F. Thackeray (Johannesburg). We thank the Editor and two anonymous reviewers for their comments. We thank the DSI-NRF for sponsoring the Micro-XCT facility at Necsa, and the DSI-NRF and the University of the Witwatersrand for funding the microfocuss X-ray CT facility in the Evolutionary Studies Institute. We acknowledge the support of the AESOP+ program, the Claude Leon Foundation, the DSI-NRF Centre of Excellence in Palaeosciences and the French Institute of South Africa. The Ghent University Special Research Fund (BOFUGent) is acknowledged for the financial support of the Centre of Expertise UGCT (BOFEXP.2017.0007). Major funding for the Sterkfontein excavations, microCT scanning work and research was provided by South African National Research Foundation grants (#82591, #82611, #98808, #129336) and by PAST. Opinions expressed and conclusions arrived at are those of the authors and are not necessarily to be attributed to the Centre of Excellence in Palaeosciences. Ethical clearance for the use of extant human crania was obtained from the Main Research Ethics committee of the Faculty of Health Sciences, University of Pretoria in February 2016.

## Competing interests

We have no competing interests to declare.

## Authors' contributions

Conceptualisation: A.B.; methodology: A.B., J.D.; data collection – excavations: R.J.C., D.S., J.L.H., T.R.P.; data collection – scanning: L.V.H., L.B.; K.J.C.; data analysis: A.B., K.C.; writing – the initial draft: A.B.; writing – revisions: A.B., D.S., R.J.C., K.J.C., J.D., L.V.H., L.B., J.L.H., T.R.P.; funding acquisition: A.B., D.S.

## References

1. Stratford DJ. A review of the geomorphological context and stratigraphy of the Sterkfontein Caves, South Africa. In: Kilmchouk A, Palmer AN, De Waele J, Auler AS, Audra P, editors. Hypogene karst regions and caves of the world. Cham: Springer; 2017. p. 879–891. <https://doi.org/10.1007/978-3-319-53348-3>
2. Partridge TC, Granger DE, Caffee MW, Clarke RJ. Lower Pliocene hominid remains from Sterkfontein. *Science*. 2003;300(5619):607–612. <https://doi.org/10.1126/science.1081651>
3. Partridge TC. Re-appraisal of lithostratigraphy of Sterkfontein hominid site. *Nature*. 1978;275:282–287. <https://doi.org/10.1038/275282a0>
4. Wilkinson MJ. Geomorphic perspectives on the Sterkfontein australopithecine breccias. *J Archaeol Sci*. 1983;10(6):515–529. [https://doi.org/10.1016/0305-4403\(83\)90034-1](https://doi.org/10.1016/0305-4403(83)90034-1)
5. Wilkinson MJ. Lower-lying and possibly older fossiliferous deposits at Sterkfontein. In: Tobias PV, editor. Hominid evolution: Past, present and future. New York: Alan R. Liss; 1985. p. 165–170. <https://doi.org/10.1525/aa.1987.89.1.02a00770>
6. Partridge TC, Watt IB. The stratigraphy of the Sterkfontein hominid deposit and its relationship to the underground cave system. *Palaeontol Africana*. 1991;28:35–40.
7. Pickering TR, Kramers JD. Re-appraisal of the stratigraphy and determination of new U-Pb dates for the Sterkfontein hominid site, South Africa. *J Hum Evol*. 2010;59(1):70–86. <https://doi.org/10.1016/j.jhevol.2010.03.014>
8. Beaudet A, Carlson KJ, Clarke RJ, De Beer F, Dhaene J, Heaton J, et al. Cranial vault thickness variation and inner structural organization in the StW 578 hominin cranium from Jacovec Cavern, South Africa. *J Hum Evol*. 2018;121:204–220. <https://doi.org/10.1016/j.jhevol.2018.04.004>
9. Bruxelles L, Clarke RJ, Maire R, Ortega R, Stratford D. Stratigraphic analysis of the Sterkfontein StW 573 *Australopithecus* skeleton and implications for its age. *J Hum Evol*. 2014;70:36–48. <https://doi.org/10.1016/j.jhevol.2014.02.014>
10. Bruxelles L, Stratford DJ, Maire R, Pickering TR, Heaton JL, Beaudet A, et al. A multiscale stratigraphic investigation of the context of StW 573 'Little foot' and Member 2, Sterkfontein caves, South Africa. *J Hum Evol*. 2019;133:78–98. <https://doi.org/10.1016/j.jhevol.2019.05.008>
11. Stratford DJ, Grab S, Pickering TR. The stratigraphy and formation history of fossil-and artefact-bearing sediments in the Milner Hall, Sterkfontein Cave, South Africa: New interpretations and implications for palaeoanthropology and archaeology. *J Afr Earth Sci*. 2014;96:155–167. <https://doi.org/10.1016/j.jafrearsci.2014.04.002>
12. Clarke RJ, Kuman K. The skull of StW 573, a 3.67 Ma *Australopithecus prometheus* skeleton from Sterkfontein Caves, South Africa. *J Hum Evol*. 2019;134:102634. <https://doi.org/10.1016/j.jhevol.2019.06.005>
13. Wood B, Doherty D, Boyle E. Hominin taxic diversity. In: Oxford Research Encyclopedias: Anthropology. Oxford University Press; 2020. <https://doi.org/10.1093/acrefore/9780190854584.013.194>
14. Pickering TR, Heaton JL, Clarke RJ, Stratford D, Heile AJ. Hominin lower limb bones from Sterkfontein Caves, South Africa (1998–2003 excavations). *S Afr J Sci*. 2021;117(1/2), Art. #6758. <https://doi.org/10.17159/sajs.2021/6758>
15. L'Abbé EN, Loots M, Meiring JH. The Pretoria Bone Collection: A modern South African skeletal sample. *Homo*. 2005;56(2):197–205. <https://doi.org/10.1016/j.jchb.2004.10.004>



16. Broom R. Discovery of a new skull of the South African apeman, *Plesianthropus*. *Nature*. 1947;159(4046):672. <https://doi.org/10.1038/159672a0>
17. Broom R, Robinson JT, Schepers GWH. Sterkfontein ape-man, *Plesianthropus*. *Transv Mus Mem*. 1950;4(4065):1–117. <https://doi.org/10.1038/160430b0>
18. Vrba ES. Early hominids in southern Africa: Updated observations on chronological and ecological background. In: Tobias PV, editor. *Hominid evolution: Past, present and future*. New York: Alan R. Liss; 1958. p. 195–200. <https://doi.org/10.1525/aa.1987.89.1.02a00770>
19. Delson E. Chronology of South African australopithecine site units. In: Grine FE, editor. *Evolutionary history of the 'robust' australopithecines*. New York: Aldine de Gruyter; 1988. p. 317–324. <https://doi.org/10.4324/9780203792667>
20. McKee JK, Thackeray JF, Berger LR. Faunal assemblage seriation of Southern African Pliocene and Pleistocene fossil deposits. *Am J Phys Anthropol*. 1995;96(3):235–250. <https://doi.org/10.1002/ajpa.1330960303>
21. Potze S, Thackeray JF. Temporal lines and open sutures revealed on cranial bone adhering to matrix associated with Sts 5 ("Mrs Ples"), Sterkfontein, South Africa. *J Hum Evol*. 2010;58(6):533–535. <https://doi.org/10.1016/j.jhevol.2009.11.005>
22. Beaudet A. Media 000405957: Calotte [Mesh] [CT] [data set]. In: Morphosource. Available from: <https://www.morphosource.org/concern/media/000405957?locale=en>
23. Avizo v9.0. Hillsboro, OR: FEI Company; 2015.
24. Rhinoceros 3D v6.0. Seattle, WA: Robert McNeel & Associates; 2010. Available from: <https://www.rhino3d.com/>
25. Cignoni P, Corsini M, Ranzuglia G. MeshLab: An open-source 3D mesh processing system. *ERCIM News*. 2008;73:47–48.
26. Durrleman S, Pennec X, Trouvé A, Ayache N, Braga J. Comparison of the endocranial ontogenies between chimpanzees and bonobos via temporal regression and spatiotemporal registration. *J Hum Evol*. 2012;62(1):74–88. <https://doi.org/10.1016/j.jhevol.2011.10.004>
27. Beaudet A, Dumoncel J, De Beer F, Duployer B, Durrleman S, Gilissen E, et al. Morphoarchitectural variation in South African fossil cercopithecoid endocasts. *J Hum Evol*. 2016;101:65–78. <https://doi.org/10.1016/j.jhevol.2016.09.003>
28. Beaudet A, Dumoncel J, Thackeray JF, Bruxelles L, Duployer B, Tenailleau C, et al. Upper third molar internal structural organization and semicircular canal morphology in Plio-Pleistocene South African cercopithecoids. *J Hum Evol*. 2016;95:104–120. <https://doi.org/10.1016/j.jhevol.2016.04.004>
29. Beaudet A, Dumoncel J, De Beer F, Durrleman S, Gilissen E, Oettlé A, et al. The endocranial shape of *Australopithecus africanus*: Surface analysis of the endocasts of Sts 5 and Sts 60. *J Anat*. 2018;232(2):296–303. <https://doi.org/10.1111/joa.12745>
30. Beaudet A, Holloway R, Benazzi S. A comparative study of the endocasts of OH 5 and SK 1585: Implications for the paleoneurology of eastern and southern African *Paranthropus*. *J Hum Evol*. 2021;156:103010. <https://doi.org/10.1016/j.jhevol.2021.103010>
31. Pan L, Dumoncel J, Mazurier A, Zanolli C. Hominin diversity in East Asia during the Middle Pleistocene: A premolar endostructural perspective. *J Hum Evol*. 2020;148:102888. <https://doi.org/10.1016/j.jhevol.2020.102888>
32. Beaudet A, Clarke RJ, Heaton JL, Pickering TR, Carlson KJ, Crompton R, et al. The atlas of StW 573 and the late emergence of human-like head mobility and brain metabolism. *Sci Rep*. 2020;10:4285. <https://doi.org/10.1038/s41598-020-60837-2>
33. Urciuoli A, Zanolli C, Almécija S, Beaudet A, Dumoncel J, Morimoto N, et al. Reassessment of the phylogenetic relationships of the late Miocene apes *Hispanopithecus* and *Rudapithecus* based on vestibular morphology. *Proc Natl Acad Sci USA*. 2021;118, e2015215118. <https://doi.org/10.1073/pnas.2015215118>
34. Braga J, Zimmer V, Dumoncel J, Samir C, De Beer F, Zanolli C, et al. Efficacy of diffeomorphic surface matching and 3D geometric morphometrics for taxonomic discrimination of Early Pleistocene hominin mandibular molars. *J Hum Evol*. 2019;130:21–35. <https://doi.org/10.1016/j.jhevol.2019.01.009>
35. Besl, PJ, McKay ND. A method for registration of 3-D shapes. *IEE Trans Pattern Anal*. 1992;14:239e256
36. Dumoncel J, Subsol G, Durrleman S, Jessel J-P, Beaudet A, Braga J. How to build an average model when samples are variably incomplete? Application to fossil data. In: *IEEE Conference on Computer Vision and Pattern Recognition Workshops*; 2016 June 27–30; Las Vegas, NV, USA. IEEE; 2016. p. 541–548. <https://doi.org/10.1109/CVPRW.2016.74>
37. Deformetric v4.0. 2014. <https://www.deformetrica.org/>
38. Lieberman DE. *The evolution of the human head*. Cambridge, MA: Harvard University Press; 2011. <https://doi.org/10.2307/j.ctvnrtrmh>
39. Ravosa MJ. Interspecific perspective on mechanical and nonmechanical models of primate circumorbital morphology. *Am J Phys Anthropol*. 1991;86(3):369–396. <https://doi.org/10.1002/ajpa.1330860305>
40. Lacruz RS, Stringer CB, Kimbel WH, Wood B, Harvati K, O'Higgins P, et al. The evolutionary history of the human face. *Nat Ecol Evol*. 2019;3(5):726–736. <https://doi.org/10.1038/s41559-019-0865-7>
41. Harvati K, Weaver TD. Human cranial anatomy and the differential preservation of population history and climate signatures. *Anat Rec A Discov Mol Cell Evol Biol*. 2006;288(12):1225–1233. <https://doi.org/10.1002/ar.a.20395>
42. Schroeder L, Roseman CC, Cheverud JM, Ackermann RR. Characterizing the evolutionary path(s) to early *Homo*. *PLoS ONE*. 2014;9(12), e114307. <https://doi.org/10.1371/journal.pone.0114307>
43. Pereira-Pedro AS, Masters M, Bruner E. Shape analysis of spatial relationships between orbito-ocular and endocranial structures in modern humans and fossil hominids. *J Anat*. 2017;231(6):947–960. <https://doi.org/10.1111/joa.12693>
44. Beaudet A, Bruner E. A frontal lobe surface analysis in three archaic African human fossils: OH 9, Buia, and Bodo. *C R Palevol*. 2017;16:499–507. <https://doi.org/10.1016/j.crpv.2016.12.002>
45. Ponce de León MS, Bienvenu T, Marom A, Engel S, Tafforeau P, Alatorre Warren JL, et al. The primitive brain of early *Homo*. *Science*. 2021;372(6538):165–171. <https://doi.org/10.1126/science.aaz0032>
46. Cameron D, Patnaik R, Sahni A. The phylogenetic significance of the Middle Pleistocene Narmada hominin cranium from Central India. *Int J Osteoarchaeol*. 2004;14(6):419–447. <https://doi.org/10.1002/oa.725>
47. Moss ML, Young RW. A functional approach to craniology. *Am J Phys Anthropol*. 1960;18(4):281–292. <https://doi.org/10.1002/ajpa.1330180406>
48. Anzelmo M, Ventrice F, Barbeito-Andres J, Pucciarelli HM, Sardi ML. Ontogenetic changes in cranial vault thickness in a modern sample of *Homo sapiens*. *Am J Hum Biol*. 2015;27(4):475–485. <https://doi.org/10.1002/ajhb.22673>
49. Bruner E, Athreya S, de la Cuetara JM, Marks T. Geometric variation of the frontal squama in the genus *Homo*: Frontal bulging and the origin of modern human morphology. *Am J Phys Anthropol*. 2013;150:313–323. <https://doi.org/10.1002/ajpa.22202>